Deciphering the Tumor Immune Microenvironment: Microscale Measurements for Precision Detection and Multidimensional Analysis

Lu Wang[1], Fan Yin[2], Rongping Luo[1], Fengqi Dong[3], Jianxin Lyu[1], Zhen Wang[4], and Yi Zhang[5]

[1]Hangzhou Medical College
[2]Zhejiang University
[3]Wenzhou Medical University
[4]Tiantai People's Hospital of Zhejiang Province
[5]Zhejiang Provincial People's Hospital

November 25, 2024

Abstract

The precision of cancer immunotherapy is critically dependent on accurately characterizing the tumor immune microenvironment (TIME), which represents a complex interplay of cellular components, cytokines, and metabolic factors. Traditional diagnostic methods have been limited in resolving the dynamic molecular interactions within the TIME at a microscale level. This review focuses on recent advancements in microscale measurements for identifying novel immune-oncology biomarkers and therapeutic targets within the TIME, emphasizing the importance of high-fidelity data on tumor immune infiltrates and the significance of longitudinal high-dimensional analysis for predicting treatment responses. Furthermore, the review discusses the impact of cancer metabolic reprogramming on the TIME and the potential of new biomarkers for predicting responses to immunotherapy. The role of nanotechnology in enhancing the detection of immune checkpoints and the development of AI-based sensors for real-time data analysis and predictive modeling is also explored, highlighting the potential of these advanced technologies to revolutionize the field of cancer immunotherapy.

Introduction

The pursuit of precision in cancer therapy is inextricably linked to the accurate detection and interpretation of the tumor immune microenvironment (TIME), a complex and dynamic arena where immune and cancer cells engage in a delicate balance[1]. Characterized by a heterogeneous array of cellular components, cytokines, chemokines, and extracellular matrix elements, this microenvironment plays a pivotal role in tumor progression and response to therapeutic interventions. The development of effective immunotherapies relies heavily on the ability to modulate this immunosuppressive environment, often regulated by complex signaling pathways and metabolic interactions, posing significant challenges[2][3].

Traditional diagnostic methods have reached their limits in resolving the nuanced molecular dynamics at the microscale, crucial for understanding the early stages of tumorigenesis and disease progression–the "butterfly effect" in TIME theranostics[4][5]. Microscale measurements, thus, emerge as a critical approach, providing an integrated assessment of the spatiotemporal and environmental contexts of tumor-immune interactions, especially at the early stage of tumorigenesis[6]. More importantly, recent advancements in nanotechnology and biomaterials science have marked a significant leap in precision tumor immunotherapy, particularly enhancing multidimensional detection capabilities[7]–[9]. Nanoscale platforms, equipped with molecular recognition

elements, offer exceptional sensitivity and selectivity for probing the TIME, enabling the visualization of biomarker distribution and monitoring dynamic changes within the microenvironment in real time[10].

In this review, we delve into the precision detection strategies addressing the multidimensional aspects of the TIME, with a focus on microscale measurements of tumor immune-related markers. By integrating analyses of key gene expressions, metabolic profiling, and direct sensing of the TIME's distinctive features, these interdisciplinary technologies offer the promise of more efficacious and personalized cancer treatments. These innovative approaches are set to redefine our understanding of the intricate interactions within the TIME, heralding a future of increasingly precise cancer therapies (Figure 1).

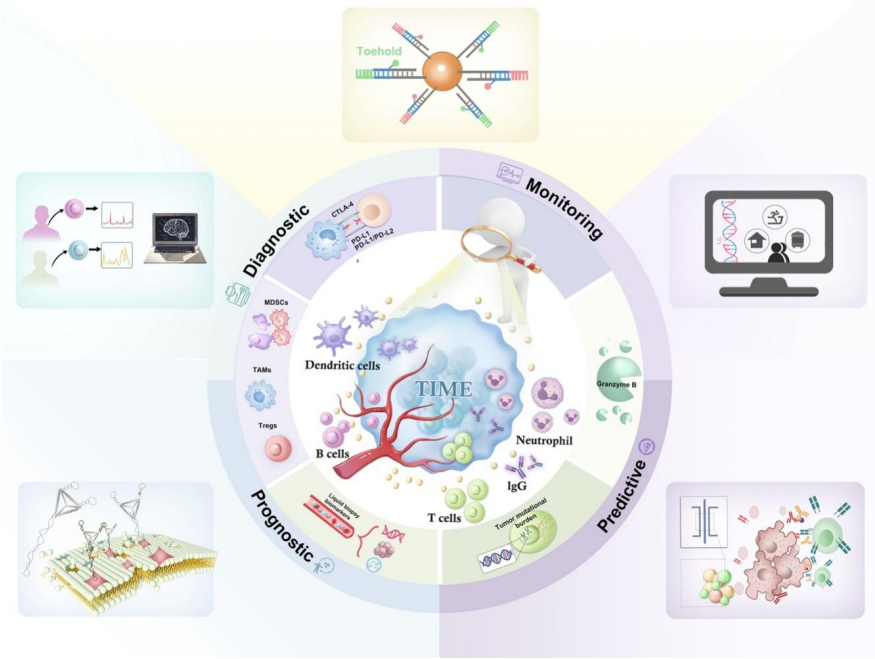

Figure 1. Schematic illustration of the microscale measurements for tumor immune microenvironment (TIME).

Unveiling the TIME through Biomarker Profiling in Cancer Immunotherapy

The TIME is a dynamic and complex ecosystem central to in the interplay between cancer progression and responses to immunotherapy[11]. Characterized by the presence of diverse immune cells, such as T cells, B cells, NK cells, tumor-associated macrophages (TAMs), dendritic cells (DCs), and myeloid-derived suppressor cells (MDSCs), the TIME actively influences immune response trajectories against tumors[12][13]. The complexity of the TIME is further amplified by the inclusion of cellular components, the extracellular matrix, and soluble factors such as cytokines and chemokines, which collectively influence immune cell behavior. Notably, cytokines such as IL-2 and IL-12 have shown potential in enhancing antitumor responses by activating and promoting the proliferation of T cells and NK cells[14]. The expression of immune checkpoint biomarkers, including programmed cell death 1 (PD-1), programmed cell death ligand 1 (PD-L1), cytotoxic T lymphocyte-associated antigen-4 (CTLA-4), lymphocyte activation gene 3 (LAG-3), and tyrosine-based inhibition motif domain (TIGIT) on immune cells, is crucial for modulating the balance between immune tolerance and activation[15]–[17]. Thus, advances in deciphering the TIME have highlighted its importance in the efficacy of cancer immunotherapies, particularly with the advent of immune checkpoint inhibitors, which have revolutionized cancer treatment by countering the mechanisms tumors employ to evade immune detection and destruction.

Unveiling the intricacies of the TIME requires meticulous microscale analysis, facilitating the discovery of novel biomarkers and therapeutic targets, as detailed in Table 1. High-fidelity data on the characteristics and quality of tumor immune infiltrates involve detailed measurements across a spectrum of immune biomarkers, including discrete immune cell populations, their spatial distribution, activation states, and the expression levels of certain molecules within the tumor microenvironment. Longitudinal high-dimensional analysis using multi-cytokines measurements has revealed that higher proportions of circulating $CD8^+$ T cells and specific subset significantly correlate with poor clinical responses to immunotherapy[18]. This granular analysis affords researchers a deeper understanding of the tumor's immune topography, enabling more precise predictions regarding the tumor's responsiveness to immune checkpoint blockade (ICB) therapy.

Table 1. Overview of the multidimensional biomarkers and therapeutic targets within the TIME through microscale analysis

Correlated with clinical responses to immunotherapy. &[38]CTLA-4 Immune checkpoint molecule that inhibits T-cell activation. Various Immunoassays, Flow cytometry. Predictive of response to immune checkpoint blockade therapy. [39]LAG-3 Immune checkpoint molecule that delivers inhibitory signals to T cells. Immunohistochemistry, Flow cytometry. Potential predictive biomarker for response to immune checkpoint inhibitors. [17]TIGIT Immune checkpoint receptor that inhibits T cell activation and function. Flow Cytometry, Immunohistochemistry. Potential predictive biomarker for response to immune checkpoint inhibitors. [15]$Exo_{PD\text{-}L1}$ Soluble form of PD-L1 found in exosomes, reflects tumor immune microenvironment. Exosome Isolation Followed by Immunoassays, Molecular imaging. Predictive biomarker for response to immunotherapy. [40]–[44]This focus on precision has been underscored by the significant efforts directed towards identifying oncological-immune biomarkers, with the immunoscore being crucial for quantifying specific immune cell populations within the tumor microenvironment at a granular spatial level[37]. Microscale measurements enable the precise detection and localization of $CD8^+$ and $CD45RO^+$ T cells, providing critical insights into the immune landscape of the tumor[11]. Combining tissue biomarkers, such as PD-L1 expression, with other tissue-based markers enhances predictive accuracy[45]. Furthermore, integrating molecular biomarkers, including tumor mutational burden (TMB) and microsatellite instability (MSI), is a pivotal strategy for refining prediction models[36][37]. The confluence of immune transcriptomic biomarkers with other markers elucidates the nuances of the immune response to immunotherapy. Circulating biomarkers, exemplified by the neutrophil-to-lymphocyte ratio (NLR) and serum cytokines, serve as complementary indicators that, in conjunction with tissue-based assessments, may enhance the precision of predictive models[38]. Microscale measurements are pivotal in unveiling the intricate heterogeneity within the TIME, providing critical insights for discerning patient cohorts likely to benefit from ICB therapy. The presence and interactions of specific immune cells, including cytotoxic and regulatory T cells, with tumor cells significantly influence the prognosis of ICB treatment. State-of-the-art techniques, including single-cell RNA sequencing (scRNA-seq)[30], multiplexed immunohistochemistry[46], and spatial transcriptomics[47], provide the necessary granularity to capture the complexity of the TIME. Among these, radiomics is particularly notable as an analytical method that translates high-resolution medical images into quantifiable data, thereby offering detailed insights into the cellular and molecular dimensions of tumors[48]. Li et al. recently introduced a radiomics score (RS) based on computed tomography (CT) as a noninvasive imaging biomarker for evaluating the TIME. This score correlates with NLR and predicts outcomes in advanced gastric cancer patients[49]. The RS, derived from selected features and their coefficients, enables the classification of patients into different risk cohorts and demonstrats an association between radiomics imaging biomarkers and treatment efficacies (Figure 2a). Building upon this, Devkota et al. investigated a nano-radiomics approach that differentiates treatment groups through texture-based features, providing a method for detecting tumor responses to cellular immunotherapy targeting MDSCs[50]. This approach highlights the potential of nanotechnology-based microscale measurements in predicting responses to immunotherapy. While scRNA-seq is a powerful tool for analyzing gene expression and measuring cellular states and heterogeneity, it captures a static snapshot of gene expression at a specific time point, lacking the dynamic changes in expression over time. Moreover, the spatial context, essential for understanding cell-cell interactions and the influence of the microenvironment, is often missing. To address these limitations, Weiner and colleagues developed Zman-seq, a time-resolved

single-cell technology that tracks gene expression dynamics in individual cells over time[30]. In the context of the TIME, Zman-seq is particularly valuable for elucidating the adaptive mechanisms of immune cells as they respond to the tumor. It provides intricate, high-resolution data on the molecular shifts within immune cells as they interact with the tumor, delineating the precise trajectories that immune cells undertake as they transition from functional to dysfunctional states (Figure 2b). This understanding can inform the development of strategies to counteract immune dysfunction, potentially leading to the design of more efficacious immunotherapies. Very recently, Wang et al. presented a groundbreaking approach to understanding the spatial predictors of immunotherapy response in triple-negative breast cancer[51]. Utilizing imaging mass cytometry, the researchers meticulously profiled the*in-situ* expression of 43 proteins across tumor samples from a clinical trial of neoadjuvant ICB therapy (Figure 2c). The findings revealed that the proliferative fractions of $CD8^{+}TCF1^{+}$ T cells and $MHCII^{+}$ cancer cells were the dominant predictors of response to ICB, with additional predictive value provided by cancer-immune interactions. The study introduced a precision medicine element by demonstrating that combining tissue features before and on-treatment could optimally predict treatment response, suggesting the potential for early biopsies to guide adaptive therapy.

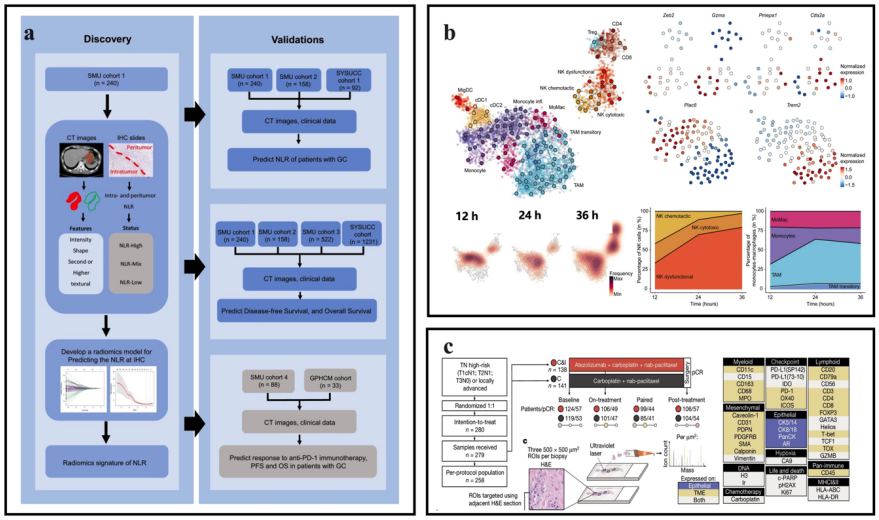

Figure 2. a) Study design for the discovery and validation of the RS imaging biomarker in gastric cancer. Reproduced under the terms of the CC BY license[49]. Copyright 2022, Springer Nature. b) Zman-seq reveals the temporal dynamics of TIME in glioblastoma including projections of gene expression in lymphocytes and myeloid cells, density enrichment of cells across time bins, and a stacked area plot illustrating the relative percentages of NK subtypes and mononuclear phagocyte populations at 12, 24, and 36 hours. Reproduced with permission[30]. Copyright 2024, Elsevier. c) The schematic representing imaging mass cytometry to profile the expression of 43 proteins at subcellular resolution in tumor samples collected from patients with TNBC. Reproduced under the terms of the CC BY license[51]. Copyright 2023, Springer Nature.

Nanotechnology-based Microscale Measurements for Predicting the Response to Cancer Immunotherapy

As previously discussed, cancer immunotherapy, which aims to modulate the immune system to combat tumors, frequently encounters challenges due to its complexity and variability, leading to low response rates. Timely and accurate monitoring of immune responses is essential for assessing treatment effectiveness. Nanotechnology-based microscale measurements have emerged as a pivotal advancement, offering non-invasive and highly sensitive diagnostic strategies personalized for individual patients[52][53]. These methods leverage the unique molecular profiles of tumors to enable personalized treatment plans that adapt to the specific dynamics of each patient's disease progression. The identification of early response biomarkers, including PD-L1, PD-1, granzyme B (GzmB), ROS, etc., provides a crucial reference for evaluating the

effectiveness of immunotherapy. The following sections provide an overview of microscale measurements of biomarkers in the immune response by optical and non-optical readouts for the evaluation of the tumor immunotherapeutic efficacy.

Optical-based Detection Methods

Molecular imaging

Real-time monitoring of immunotherapy in tumors via imaging methods is significant for promptly assessing treatment effectiveness and optimizing clinical strategies. Molecular imaging is a non-invasive technique that uses the interaction of light with biological tissues to visualize and quantify molecular biomarkers[54]. Various imaging modalities, including radionuclide imaging (PET and SPECT)[55], molecular magnetic resonance imaging (mMRI)[56], magnetic resonance spectroscopy (MRS)[57] and optical imaging (bioluminescence and fluorescence), provide distinct insights into biological processes. Photoacoustic (PA) imaging, which generates images based on the heat generated from light absorption, offers a unique perspective on tissue morphology and function[58]. In cancer immunotherapy, these techniques are particularly valuable for monitoring immune activation, with nanoprobes designed to target specific immune biomarkers enhancing imaging sensitivity and specificity. This allows for real-time monitoring of the immune system's interaction with the tumor, facilitating a more precise assessment of therapeutic efficacy.

GzmB, an enzyme involved in the immune killing effect, is a pivotal biomarker for real-time monitoring of immune activation and tumor apoptosis. Its peptide substrate can be conjugated with fluorescent dyes or contrast agents to create GzmB-activated imaging probes[32]. These probes, using modalities such as PET, bioluminescence, or fluorescence imaging, deomonstrate high specificity and accuracy in detecting GzmB activity. Kulkarni and colleagues developed a GzmB nanoreporter (GNR) for the early monitoring of tumor responses to immunotherapy[34]. These GNRs are designed to deliver a PD-L1 antibody to the tumor site and track GzmB activity, thereby monitoring effective immune responses. The study shows that GNRs can monitor the initiation of effective immune responses by detecting T cell-mediated GzmB release using an activatable imaging probe. By conjugating a GzmB-activatable probe to the GNRs, researchers can selectively detect enzyme functions with high signal-to-noise ratios, thereby minimizing false positives (Figure 3a). Importantly, this innovative approach allows for real-time monitoring of immunotherapy responses in tumor-bearing mice, distinguishing between highly responsive and poorly responsive tumors. Further, the same group designed a dual-sensing nanoreporter for dynamic and high-throughput monitoring of immune checkpoint inhibitor responses in tumor-derived organoids[59]. This system is engineered to capture the activities of both GzmB and caspase 3, two key proteases involved in T cell-mediated cell death. By incorporating 3D tumor-derived organoids and *ex vivo* cultures on microfluidic devices, the nanoreporter facilitates high-throughput screening of various immune checkpoint inhibitors and their combinations, providing insights into immunotherapy assessments (Figure 3b). In another study on GzmB fluorescence imaging, Xu et al. developed a "dual quenched" nanoparticle, Cy5.5-CBT-NPs, that activates fluorescence upon cleavage by GzmB to monitor the activity of CTLs in cancer immunotherapy[60]. The nanoparticle is designed as a self-assembled of a smart small molecule fluorescence probe, initially quenched. Upon interaction with GzmB, the nanoparticles disassemble, leading to fluorescence signal activation (Figure 3c).

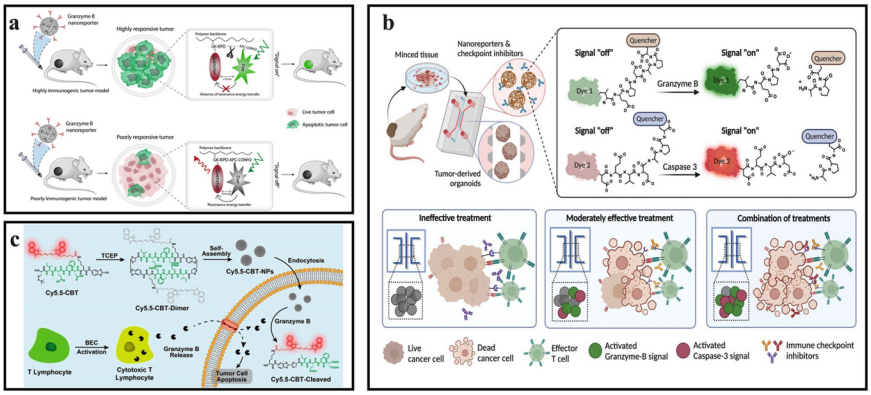

Figure 3. a) Schematics of the real-time monitoring mechanism of cytotoxic T lymphocyte activity using GNRs. Reproduced under the terms of the CC BY-NC license[34]. Copyright 2020, American Association for the Advancement of Science. b) Schematics showing the dual-probe stimuli-responsive nanoreporters' design enables high throughput screening of tumor-derived organoids response to ICB. Reproduced with permission[59]. Copyright 2024, John Wiley and Sons. c) Schematic illustration depicting the preparation of fluorescence "dual quenched" Cy5.5-CBT-NPs and the application of these nanoparticles for imaging the tumoricidal activity of cytotoxic T lymphocytes. Reproduced with permission[60]. Copyright 2022, American Chemical Society.

PET, an imaging technique utilizing radioisotopes, is gaining popularity in cancer immunotheranostics due to its high resolution and penetrating power. For example, combining PET and CT imaging technologies can predict PD-1/PD-L1 expression in tumors based on differences in glucose metabolism, monitor early metabolic changes in primary tumors, and assess immune-related adverse events due to excessive immune system activation, providing important value for evaluating short-term efficacy and long-term prognosis of immunotherapy[26]. Fu and colleagues developed two PET probes emphasizing the importance of microscale measurements of GzmB for monitoring early responses to immunotherapy and demonstrating their potential in evaluating treatment efficacy[61]. These probes are based on an intramolecular cyclization scaffold that, upon recognizing GzmB and glutathione, undergoes intramolecular cyclization and self-assembles into nanoaggregates. This process enhances probe retention at the target site, enabling accurate molecular-level detection of GzmB. The probes were utilized in a 4T1 tumor-bearing mouse model to evaluate the early response to immunotherapy (Figure 4). The results demonstrated significantly higher tumor uptake in mice treated with the immunotherapy drug compared to untreated controls, indicating the probes' potential for evaluating the efficacy of immunotherapy.

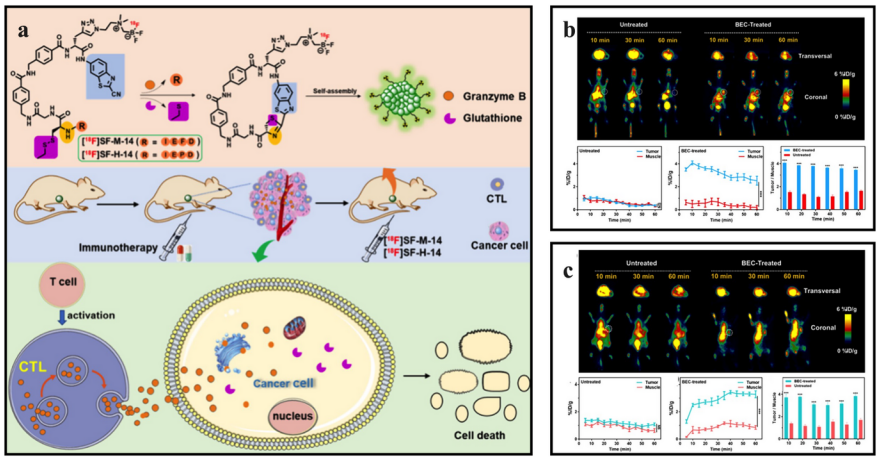

Figure 4. GzmB-targeted PET probes for monitoring tumor early response to immunotherapy a) Design scheme for the proposed probes. b) and c) PET imaging of the two probes in 4T1 tumor-bearing mice with and without immunotherapy. Reproduced with permission[61]. Copyright 2024, American Chemical Society.

Beyond GzmB, the precise detection of immune checkpoints such as PD-L1 is facilitated by molecular imaging, advancing cancer diagnostics and therapeutics. Meir et al. introduced a novel theranostic nanoparticle conjugated with anti-PD-L1, offering diagnostic imaging and therapeutic capabilities[19]. The gold nanoparticle core serves as a CT imaging contrast agent, enabling noninvasive tracking of nanoparticle distribution and tumor accumulation (Figure 5a). Notably, they found a critical correlation between CT signal intensity at 48 hours and tumor growth inhibition, linked to T cell infiltration into tumor tissue. This suggests that the imaging approach can serve as a proxy for immune response assessment. Furthermore, Tian et al. presented the development of a nanohybrid cerasome for dual-modality imaging (near-infrared fluorescence (NIRF) and MRI), enabling non-invasive, high-resolution detection of PD-L1 expression in tumors[21]. The integration of microscale measurements with dual-modality imaging and targeted therapy in this study exemplifies the potential for precision detection and multidimensional analysis of the TIME (Figure 5b).

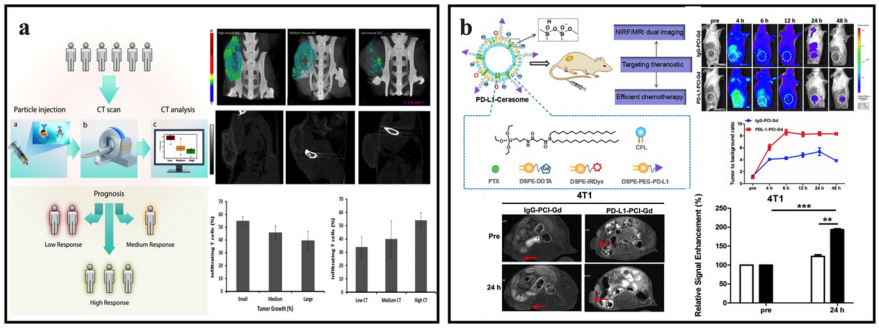

Figure 5. a) Gold nanoparticles linked to anti-PDL1 are injected systemically, allowing for CT scan analysis at 48 hours to predict immune response by assessing tumor signal intensity and categorizing subjects into high, medium, or low responders, with high responders anticipated to show sustained T-cell infiltration and tumor growth inhibition post-treatment. Reproduced with permission[19]. Copyright 2017, American Chemical Society. b) Schematics of nanoprobes constructs, followed by in vivo and ex vivo fluorescence imaging in mice bearing 4T1 tumors, comparing tumor-to-background ratios. It also includes magnetic characterization and MRI assessments of these nanoparticles, with T1-weighted images and quantified signal enhancement 24 hours post-injection, indicated by red arrows on the tumors. Reproduced with permission[21]. Copyright 2018, Elsevier.

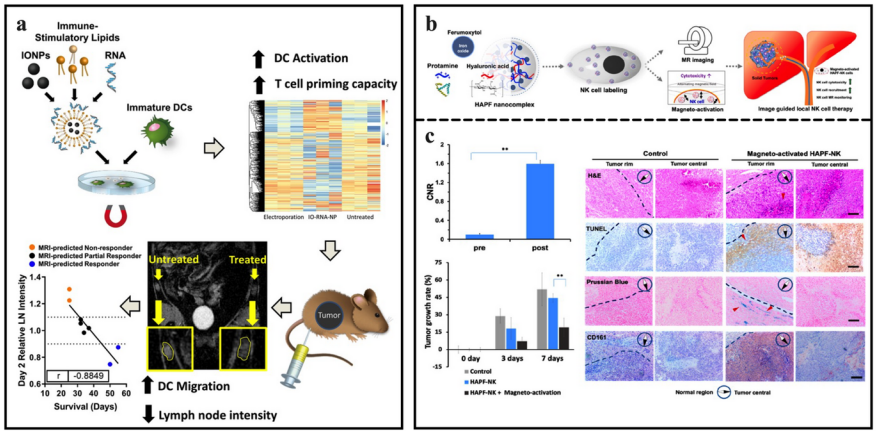

Previous report has suggested that dendritic cell (DC) migration to vaccine-site draining lymph nodes (VDLNs), as assessed by SPECT/CT, may provide an early biomarker of overall survival in glioblastoma patients treated with RNA-pulsed DC vaccines[62]. To extend the clinical utility of this biomarker, Grippin et al. introduced an innovative approach utilizing DC-activating magnetic nanoparticles for the early prediction of antitumor responses via MRI[63]. These multifunctional, RNA-loaded magnetic liposomes are designed not only to initiate potent antitumor immunity but also to serve as an early biomarker for treatment response. The inclusion of iron oxide in these nanoparticles enhances DC transfection and enables tracking of DC migration using MRI. The study demonstrates a strong correlation between T_2 *-weighted MRI intensity in lymph nodes and DC trafficking, providing an early predictor of antitumor response (Figure 6a). Moreover, Sim et al. designed a multifunctional magnetic nanocomplex to enhance NK cell-based treatments for solid tumors, effectively labeling NK cells for activation through magneto-mechanical stimulation and precise MRI monitoring[64]. This method addresses the multidimensional challenges associated with NK cell therapy, including the immunosuppressive effects of the TIME, poor tumor trafficking, and infiltration issues. The precision of this technique lies in its ability to deliver a localized, high dose of activated NK cells directly to the tumor site through transcatheter intra-arterial infusion, while simultaneously employing MRI for real-time tracking and assessment of cell distribution. The innovative use of an external magnetic field to trigger NK cell activation on-demand, combined with the enhanced MRI contrast provided by nanocomplexes, presents a non-invasive and highly controlled strategy for cancer treatment (Figure 6b).

Figure 6. a) Illustration of nanoparticle synthesis by merging iron oxide nanoparticles with tumor antigen-encoding mRNA and specialized lipids for efficient mRNA delivery and DC activation, resulting in enhanced DC activation and T-cell stimulation, as well as MRI-trackable DC migration to lymph nodes associated with prolonged survival in mouse tumor models. Reproduced with permission[63]. Copyright 2019, American Chemical Society. b) Schematics of nanocomplexes for efficient labeling, magneto-activation, and MRI imaging of NK cells, enabling MR image-guided local NK cell therapy to address challenges in solid tumor treatment. c) The increased Contrast-to-Noise ratio in MRI T_2 * images before and after the infusion of NK cells, reduced tumor growth following magneto-activation of nanocomplex labeled-NK cells, and corresponding histological analyses of tumor tissues, indicating significant therapeutic effects. Reproduced with permission[64]. Copyright 2021, American Chemical Society.

The integration of functional nucleic acids (FNA), leveraging their specific recognition capabilities and DNA-assisted nanomaterial assembly, provides a robust platform for constructing sensitive and versatile imaging platforms[65]. For example, to accurate analyze exosomal PD-L1 ($Exo_{PD\text{-}L1}$), a predictive biomarker for immunotherapy response, Huang et al. introduced the HOLMES-$Exo_{PD\text{-}L1}$ method, which utilizes an evolved aptamer for selective PD-L1 binding[66]. This method, when coupled with homogeneous thermophoresis, achieves rapid binding kinetics, surpassing conventional ELISA methods in terms of sensitivity, speed, and ease of operation (Figure 7a). Yang and colleagues developed a dual-cycling nanoprobe (DCNP) for the simultaneous detection of exosomal miRNA-21 and $Exo_{PD\text{-}L1}$directly in exosome lysates[44]. The DCNP, featuring a DNA molecular machine-based design, enables signal-amplified synchronous response to both targets. This results in with high sensitivity and accuracy in differentiating breast cancer patients from healthy individuals (Figure 7b). Moreover, Chen et al. presented a novel approach integrating FNA for the precise quantification of $Exo_{PD\text{-}L1}$ protein[20]. This approach develops a signal amplification method that utilizes aptamer recognition and DNA scaffold hybridization-triggered assembly of quantum dot nanospheres, enabling dual-color phenotyping of exosomes for the distiction between cancer patients and healthy individuals from a small blood sample, as well as the prediction of immunotherapy outcomes.

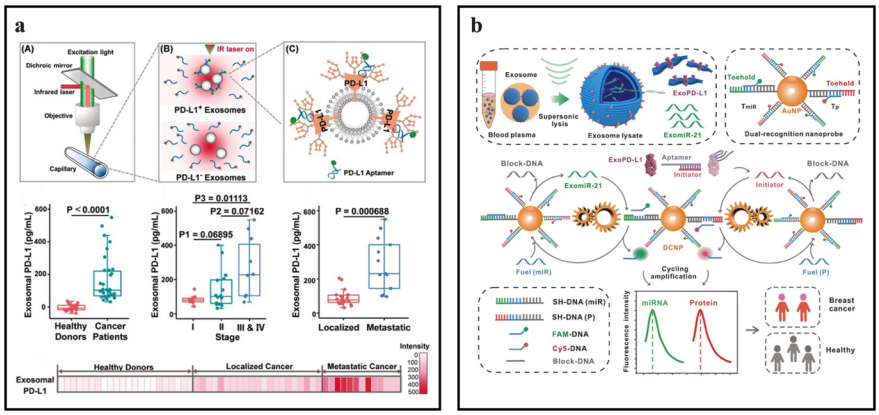

Figure7. a) The HOLMES-ExoPD-L1 analysis involves using an infrared laser in a capillary to detect exosomal PD-L1 expression levels, with a distinct fluorescence signal from aptamer-antigen complexes, allowing for precise discrimination between PD-L1 positive and negative exosomes in plasma samples from healthy donors and cancer patients across various stages and conditions. Reproduced with permission[66]. Copyright 2020, John Wiley and Sons. b) The DCNP strategy for the concurrent detection of exosomal PD-L1 and miR-21 in blood plasma through supersonic lysis of plasma exosomes and the use of a dual recognition nanoprobe on an AuNP surface, enabling breast cancer diagnosis. Reproduced with permission[20]. Copyright 2022, Elsevier.

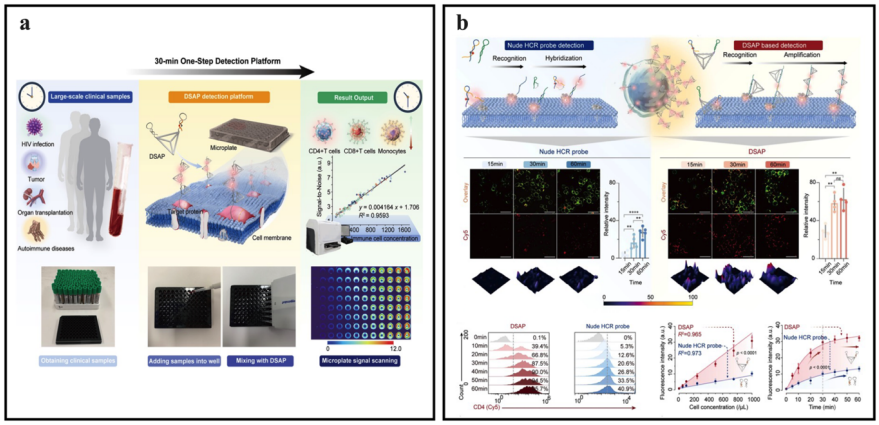

Recently, Chen et al. developed a DNA framework signal amplification platform that utilizes optimized aptamers and DNA tetrahedral framework-based probes, achieving high-sensitivity detection of various immune cells, including $CD4^+$, $CD8^+$, T-lymphocytes, and monocytes, with an impressive limit of detection down to 1/100 μL[67]. This platform enables one-step immune-cell phenotyping within 30 minutes, significantly reducing detection time and cost compared to traditional flow cytometry. This high-throughput immune monitoring system exhibits excellent diagnostic accuracy in staging immunodeficiency for HIV patients, indicating a promising avenue for the development of point-of-care devices, and holds potential to revolutionize mass health screenings through rapid, sensitive, and cost-effective immune profiling (Figure 8). The integration of this platform into multidimensional TIME analysis underscores its potential to enhance the precision of cancer immunotherapy strategies by simultaneous assessing various immune cell subsets and their functional states.

Figure 8. a) The DSAP-based platform for high-throughput immune monitoring offers a simplified, one-step procedure with a detection time of under 30 minutes, enabling rapid and sensitive analysis of diverse

immune cell numbers in large sample batches. b) The comparison between DSAP and nude HCR probes for detecting membrane proteins, presenting CLSM images of HuT-78 cells at various time points, FCA over a 60-minute interval, and MFI measurements at different cell concentrations, demonstrating the superior performance of DSAP in terms of fluorescence intensity and signal stability. Reproduced under the terms of the CC BY license[67]. Copyright 2024, Springer Nature.

Furthermore, current research has cast light on the complex interplay of diverse metabolic pathways and the pivotal role of altered metabolite levels in shaping not only cancer behavior but also the responsiveness to metabolically targeted therapies. The capacity for *in vivo* quantitative measurement of these metabolic dynamics is, therefore, a critical asset in dissecting the metabolic underpinnings of cancer cells during their proliferative and invasive processes[68]. By leveraging photoluminescence bioimaging in the near-infrared IIb (NIR-IIb) window, Fang et al. developed a novel imaging method that dynamically visualizes sO_2 levels, revealing a positive correlation between tumor-associated-vessel sO_2 levels and the basal oxygen consumption rate of cancer cells during early tumorigenesis[69]. This discovery suggested that cancer cells actively modulate their metabolic microenvironment. Furthermore, the technique was employed to demonstrate that a positive therapeutic response to ICB was associated with a significant decrease in tumor-associated-vessel sO_2 levels. The innovative aspect of this research lies in the two-plex dynamic NIR-IIb imaging, which simultaneously observes sO_2 and PD-L1, enhancing the precision of immunotherapy response prediction.

Other Optical-Based Detection Methods

In addition to molecular imaging, which often requires labeling or contrast enhancement, other optical-based detection methods like Surface-Enhanced Reman Scattering (SERS) and Surface Plasmon Resonance (SPR) offer a label-free alternative. They harness optical phenomena at metal surfaces to enhance signals, providing sensitive tools for tumor immunotherapy measurement[70][71]. These methods are instrumental throughout the development and screening of therapeutic agents, as well as in monitoring individual patients' treatment responses.

T cells, reflecting the immune response to cancer, can serve as a liquid biopsy to detect and predict responses to immunotherapy due to their direct interaction with the tumor and their ability to carry molecular information about the TIME. Ganesh et al. introduced a SERS-based approach for lung cancer diagnosis, mapping the bidirectional immune-tumor dialogue with high precision[72]. The innovative T-sense nanosensor, fabricated through multiphoton ionization, enhances the detection of molecular signatures from tumor-associated T cells, as analyzed by SERS. This technique reveals distinct immune interaction profiles of primary and metastatic lung cancers, providing molecular and phenotypic differenitation between patient-derived T cells and healthy samples (Figure 9a). The integration of machine learning algorithms with SERS data further refines diagnostic accuracy, achieving remarkable specificity and sensitivity in discriminating lung cancer stages.

Soluble PD-L1 in peripheral blood (sPD-L1), which originates from cell membrane shedding and secretion, has emerged as a potential indicator for predicting responses to cancer immunotherapy[73]. The Trau group introduced anisotropic Au-Ag alloy nanoboxes as SERS substrates, showcasing their potential for signal amplification in detecting sPD-L1 in physiological environment[74]. Utilizing SERS technology, the same group further developed a nanophotonic immunoarray for the quantitative detection of sPD-L1 in human plasma samples[23]. By electrochemically roughening gold sensor surfaces, the sensor achieves a detection sensitivity of 1 pg mL^{-1}, which is two orders of magnitude more sensitive than ELISA, highlighting its potential for early identification of patients likely to respond to immunotherapy (Figure 9b). Zhou et al. introduced another SERS-based immunoassay for the highly sensitive and specific detection of $Exo_{PD\text{-}L1}$[43]. The methodology leverages the non-selective trapping effect of Ti_3C_2Tx MXene, exploiting the affinity of Ti–O and Ti–F surface terminations with phosphate groups on the exosome membrane, thereby facilitating indiscriminate capture of exosomes. This is coupled with the selective recognition of peptide-functionalized Au@MPBA@SiO_2 SERS tags for $Exo_{PD\text{-}L1}$, further enhancing the detection's sensitivity and reliability.

Additionally, Hu et al. developed a highly SPR assay[75]. This assay utilizes a soluble intracellular binding

peptide for sPD-L1, effectively bypassing steric hindrance during immobilization on gold films and achieving signal amplification for sensitive detection (Figure 9c). Recently, Lin et al. introduced a NIRF-enhanced SPR for the detection of sPD-L1 and soluble intercellular adhesion molecule-1 (sICAM-1)[27]. This innovative assay capitalizes on the synergistic effect of gold nanostructures and a novel NIRF fluorophore to amplify the fluorescence signal. The multiplexed enhanced fluorescence microarray immunoassay (eFMIA) allows for the simultaneous and semi-quantitative detection of PD-L1 and ICAM-1. The high sensitivity and specificity of eFMIA surpass those of traditional fluorescence immunoassays and enzyme-linked immunosorbent assays, offering a significantly lower detection limit (Figure 9d). Concurrently, Wang et al. developed a nanoplasmonic sandwich immunoassay using SPR for the detection and profiling of $Exo_{PD\text{-}L1}$[41]. This method employs gold-silver core-shell nanobipyramids and gold nanorods to form immune complexes with exosomes, enabling rapid and sensitive identification of PD-L1 subtypes and offering a transformative diagnostic tool for early cancer detection, prognosis, and post-treatment monitoring.

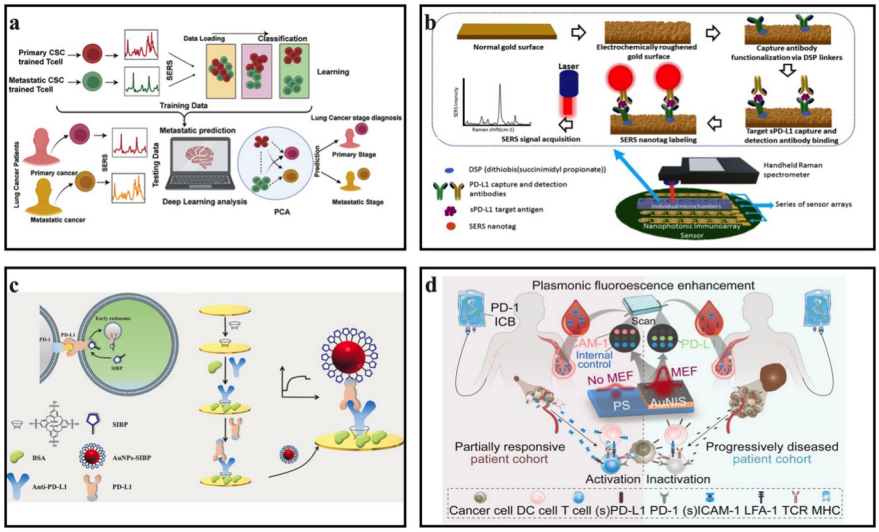

Figure 9. a) Schematics of the development of the ultrasensitive T-sense nanosensor utilizing multiphoton ionization and machine learning models to detect immune-diagnostic signatures from T cells interacting with lung cancer tumor microenvironments. Reproduced with permission[72]. Copyright 2023, American Chemical Society. b) Illustrations of the nanophotonic immunoarray sensor designed for high-throughput SERS immunoassays. Reproduced with permission[23]. Copyright 2023, Royal Society of Chemistry. c) Design of the natural peptide-based strategy for PD-L1 degradation in cancer cells and the corresponding schematic of a simple immune SPR sensor for detecting soluble PD-L1. Reproduced with permission[75]. Copyright 2021, Elsevier. d) The illustration of the NIRF-enhancing plasmonic microarray for simultaneous detection of serum ICAM-1 and PD-L1. Reproduced with permission[27]. Copyright 2023, Elsevier.

Non-Optical Methods

Electrochemical biosensors, featuring modified electrode surfaces with bioactive sensing elements, represent a detection methodology based on electrochemical reactions. The integration of these sensors into clinical diagnostics has been increasing, particularly for identifying tumor biomarkers[76]. The application of electrochemical biosensors in tumor immunotherapy assessment has expanded, with their high-sensitivity detection capabilities for biomarker fluctuations facilitating early and accurate tumor diagnosis. The miniaturization of these sensors facilitates their integration into portable devices, thereby enabling point-of-care testing (POCT) and continuous monitoring. Du et al. presented an electrochemical biosensor for tumor immunotherapy assessment that utilizes a molybdenum disulfide and multi-wall carbon nanotubes nanocomposite-modified electrode, coupled with a PD-L1 antibody-quantum dot conjugate for dual optical and electrochemical

signaling[77]. This approach not only provides a highly sensitive and selective method for detecting PD-L1 in various tumor cell types and tissues but also allows for real-time, in-situ monitoring of PD-L1 levels, a feature particularly valuable for evaluating the dynamics of immunotherapy responses (Figure 10a). Xia et al. further advanced the field by introducing an ultrasensitive electrochemical sensor that capitalizes on the synergistic effect of Ag@MXene, a two-dimensional conductive material, and an antifouling cyclic multifunctional peptide for PD-L1 detection[24]. This sensor demonstrates a broad dynamic response range and an impressively low detection limit of 24.54 pg mL^{-1}. Cao et al proposed an innovative electrochemical biosensing method that leverages DNA amplification-responsive metal-organic frameworks (PVP@HRP@ZIF-8) for the precise detection of PD-L1 positive exosomes in breast cancer[78]. Based on the principle of hyperbranched rolling circle amplification, this method induces a decrease in environmental pH, triggering the disassembly of the pH-responsive framework and the release of horseradish peroxidase, which subsequently catalyzes an electrochemical reaction for the detection of target exosomes. Notably, the method has been applied to clinical analysis, revealing elevated levels of circulating PD-L1 positive exosomes in the serum of breast cancer patients, especially those with metastatic disease (Figure 10b).

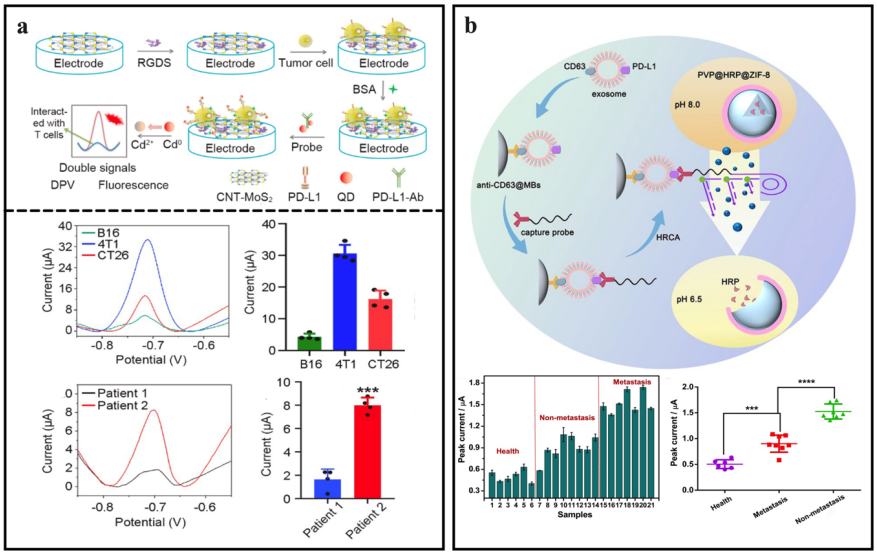

Figure 10. a) The construction of a PD-L1 electrochemical biosensor, demonstrating the interaction between tumor cells and activated T cells through PD-1, which leads to a reduced PD-L1-QD probe binding and a subsequent decrease in electrochemical signal (upper), with detection and quantification of peak currents from B16-, 4T1-, and CT26-derived tumors (lower). Reproduced with permission[77]. Copyright 2022, Elsevier. b) Illustrations of the identification of PD-L1-positive exosomes using HRCA-responsive PVP@HRP@ZIF-8, alongside a comparison of peak currents from electrochemical responses in clinical serum samples, including healthy controls and patients with non-metastatic and metastatic breast cancer. Reproduced with permission[78]. Copyright 2020, Elsevier.

Building upon these advancements, Niedziałkowski et al. introduced an electrochemical biosensor modified with the BMS-8 compound for selective interaction with PD-L1, enabling the detection of soluble PD-L1 within a concentration range of 10^{-18} to 10^{-8}M[79]. This sensor demonstrates clinical utility by distinguishing PD-L1 from other proteins such as PD-1, CD160, and BTLA, which is crucial for preventing misdiagnosis in complex biological samples. Zhang et al. presented a digital microfluidic device integrating an electrochemical sensor with a 3D matrix for the ultrasensitive detection of sPD-L1. This device, which synergizes a conductive 3D matrix composed of reduced graphene oxide, bovine serum albumin, and glutaraldehyde, enhances target capture and electrical conductivity while minimizing non-specific binding. The integration of this matrix with electrochemical sensors enables the detection of sPD-L1 at concentrations as low as 1 pg

mL^{-1} with high specificity. The platform automates sample processing and detection within a single, compact system, demonstrating the capability to analyze complex biofluids, such as breast cancer cell culture media, thereby directly reflecting the multidimensional aspects of the TIME. Similarly, Zhou and colleagues employed enzyme-catalyzed reactions to enhance the sensitivity of sPD-L1 detection[28]. The sensor integrates multiwalled carbon nanotubes for enhanced aptamer immobilization and signal amplification, coupled with covalent organic frameworks-gold nanoparticles-antibody-horseradish peroxidase for target recognition and enzymatic redox cycling. This synergistic approach amplifies the electrical signal and provides a platform for antibody and enzyme loading, resulting in a detection limit as low as 0.143 pg mL^{-1}.

Magnetic separation detection also serves as a valuable adjunct in tumor immunotherapy assessment, facilitating the precise and efficient isolation of exosomes and other magnetically labeled biological entities from complex samples[80][81]. Zhang et al. presented a groundbreaking approach integrating quantum dot nanospheres with aptamer recognition and DNA scaffold hybridization for high-precision detection of $Exo_{PD\text{-}L1}$[20]. This method is distinguished by its innovative signal amplification strategy, harnessing the synergistic effects of two aptamers to enable ultrasensitive detection of exosomal antigens. Meanwhile, the authors adeptly employ a machine-learning algorithm to classify and predict outcomes based on the spectral phenotype of exosomes, facilitating the differentiation between cancer patients and healthy individuals with remarkable accuracy (Figure 11).

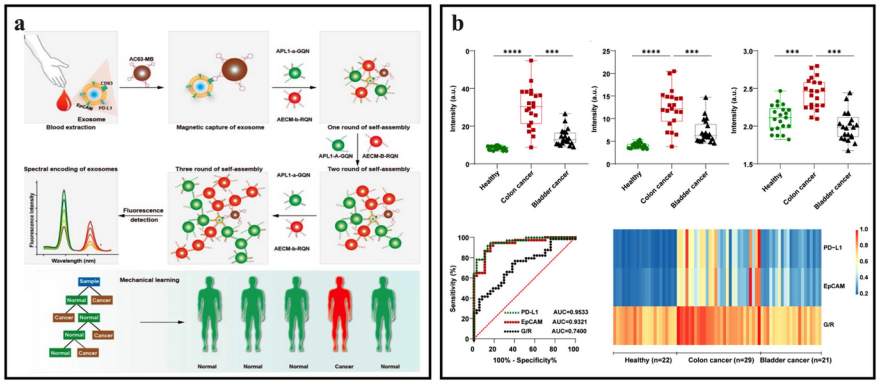

Figure 11. a) The experimental principle for exosome detection, featuring a DNA-assisted QD fluorescent nanospheres assembly amplification strategy and machine learning algorithms for diagnosing patients and predicting immunotherapy suitability, with specific nanomagnetic beads and QNs modifications indicated. b) The analysis of clinical samples, showing statistics of fluorescence intensity at 525 nm and 620 nm, the ratio of these intensities, and their diagnostic abilities assessed through ROC curve analysis, with results displayed as a heat map. Reproduced with permission[20]. Copyright 2024, American Chemical Society.

Recently, artificial intelligence (AI) has emerged as a transformative force in cancer immunotherapy, providing novel insights and predictive capabilities that are reshaping the landscape of personalized medicine[82]. The integration of AI with high-throughput sequencing, medical imaging, and omics data has enabled the development of sophisticated computational models capable of predicting treatment responses with remarkable accuracy. These models are designed to decipher the complexity of the TIME and to identify patients most likely to benefit from immunotherapeutic interventions.

In the realm of neoantigen recognition, AI algorithms have demonstrated substantial proficiency in predicting the immunogenicity of tumor-specific mutations. These neoantigens, derived from somatic mutations, are crucial for eliciting an effective T-cell response against cancer cells[83]. AI-driven approaches have been instrumental in identifying potential neoantigens from next-generation sequencing data, thereby facilitating the design of personalized cancer vaccines and T-cell therapies. For instance, deep learning models like NetMHC and MHCflurry have been trained on extensive datasets of peptide-MHC binding affinities to accurately predict the presentation of neoantigens on the cell surface-a critical step for T-cell recognition[84]. The

design of therapeutic antibodies has also been revolutionized by AI, with machine learning algorithms capable of optimizing antibody sequences for enhanced target binding and improved pharmacological properties[85]. These algorithms sift through vast sequence spaces to identify antibodies with desired characteristics, such as high affinity, reduced immunogenicity, and favorable biophysical properties. For example, deep neural networks have been employed to predict the binding affinity of antibodies to their targets, enabling the rational design of antibodies tailored for cancer therapy[86].

Furthermore, AI has been applied to predict responses to immunotherapy by analyzing multimodal data, including clinical, genomic, and radiomic information. These predictive models can stratify patients into responders and non-responders, allowing for more precise treatment planning and potentially improving outcomes. Notable examples include the use of convolutional neural networks (CNNs) to analyze histopathological images for the presence of tumor-infiltrating lymphocytes, which have been correlated with positive responses to immunotherapy[87][88]. Additionally, AI-based radiomics analysis of medical images, such as CT and MRI scans, has empowered non-invasive methods to assess the tumor microenvironment and predict treatment efficacy[89].

Conclusions and Perspectives

The landscape of cancer immunotherapy is being reshaped by the advent of nanotechnology-based microscale measurements, offering unprecedented sensitivity and specificity in detecting a wide array of immune biomarkers. These innovative approaches have not only expanded the range of detectable biomarkers but also enhanced our ability to monitor the dynamic and metabolic interactions within the TIME.

Looking to the future, the development of additional immune-oncology biomarkers and the methods to detect them will be instrumental in creating a comprehensive picture of the TIME. This will facilitate the identification of novel therapeutic targets and stratify patients into more homogeneous subgroups, thereby personalizing treatment strategies to maximize efficacy and minimize side effects. Ongoing research into the metabolic reprogramming of cancer cells and its impact on the immune response underscores the importance of expanding our molecular detection toolkit to encompass a wider array of metabolic and oxidative stress biomarkers. Furthermore, the integration of AI in sensor technology is set to usher in a new era of intelligent diagnostics, where real-time data analysis and predictive modeling could significantly expedite the clinical decision-making process. AI-based sensors have the potential to process complex biological data with unparalleled speed and accuracy, allowing for the immediate identification of treatment responders versus non-responders and the adaptation of therapeutic strategies in real-time.

In summary, nanotechnology empowered-microscale measurements in the field of cancer immunotheranostics are paving the way for a new generation of diagnostics that are not only highly sensitive and specific but also intelligent and proactive. These advancements are poised to transform our approach to cancer therapy, bringing us closer to the goal of precision medicine and, ultimately, towards more effective and personalized treatment strategies that can conquer cancer.

Acknowledgement

The work was supported in part by the Research Project of the key Project of Science and Technology of Zhejiang Province in China(2022C03024) and the project from Seeking Truthful Talents Projects of Hangzhou Medical College (00004E1RCYJ2408).

Conflict of Interest

The authors declare no conflict of interest.

References

[1] M. Binnewies, E.W. Roberts, K. Kersten, V. Chan, D.F. Fearon, M. Merad, L.M. Coussens, D.I. Gabrilovich, S. Ostrand-Rosenberg, C.C. Hedrick, R.H. Vonderheide, M.J. Pittet, R.K. Jain, W. Zou, T.K. Howcroft, E.C. Woodhouse, R.A. Weinberg, M.F. Krummel, *Nat Med* **2018** , *24* , 541.

[2] A. Hu, L. Sun, H. Lin, Y. Liao, H. Yang, Y. Mao, *Signal Transduct Target Ther* **2024** , *9* , 68.

[3] X. Xiang, J. Wang, D. Lu, X. Xu, *Signal Transduct Target Ther* **2021** , *6* , 75.

[4] M.A. Walling, J.R.E. Shepard, *Chem Soc Rev* **2011** ,*40* , 4049.

[5] H. Yu, O. Alkhamis, J. Canoura, Y. Liu, Y. Xiao,*Angewandte Chemie - International Edition* **2021** ,*60* , 16800.

[6] K.J. Hiam-Galvez, B.M. Allen, M.H. Spitzer, *Nat Rev Cancer* **2021** , *21* , 345.

[7] R. Cheng, H.A. Santos, *Adv Healthc Mater* **2023** ,*12* , 1.

[8] X. Dong, S. Xia, S. Du, M.-H. Zhu, X. Lai, S.Q. Yao, H.-Z. Chen, C. Fang, *ACS Cent Sci* **2023** , *9* , 1864.

[9] M.S. Goldberg, *Nat Rev Cancer* **2019** , *19* , 587.

[10] A. Nguyen, S. Kumar, A.A. Kulkarni, *Small Methods* **2022** , *6* , 1.

[11] J.M. Taube, J. Galon, L.M. Sholl, S.J. Rodig, T.R. Cottrell, N.A. Giraldo, A.S. Baras, S.S. Patel, R.A. Anders, D.L. Rimm, A. Cimino-Mathews, *Modern Pathology* **2018** , *31* , 214.

[12] S. Chen, A.F.U.H. Saeed, Q. Liu, Q. Jiang, H. Xu, G.G. Xiao, L. Rao, Y. Duo, *Signal Transduct Target Ther* **2023** ,*8* , 207.

[13] S.A. Lasser, F.G. Ozbay Kurt, I. Arkhypov, J. Utikal, V. Umansky, *Nat Rev Clin Oncol* **2024** , *21* , 147.

[14] D.J. Propper, F.R. Balkwill, *Nat Rev Clin Oncol* **2022** , *19* , 237.

[15] W. Tang, J. Chen, T. Ji, X. Cong, *Cell Death Dis* **2023** , *14* , 466.

[16] D.B. Doroshow, S. Bhalla, M.B. Beasley, L.M. Sholl, K.M. Kerr, S. Gnjatic, I.I. Wistuba, D.L. Rimm, M.S. Tsao, F.R. Hirsch, *Nat Rev Clin Oncol* **2021** , *18* , 345.

[17] V. Aggarwal, C.J. Workman, D.A.A. Vignali, *Nat Immunol* **2023** , *24* , 1415.

[18] E.L.-H. Leung, R.-Z. Li, X.-X. Fan, L.Y. Wang, Y. Wang, Z. Jiang, J. Huang, H.-D. Pan, Y. Fan, H. Xu, F. Wang, H. Rui, P. Wong, H. Sumatoh, M. Fehlings, A. Nardin, P. Gavine, L. Zhou, Y. Cao, L. Liu,*Nat Commun* **2023** , *14* , 5115.

[19] R. Meir, K. Shamalov, T. Sadan, M. Motiei, G. Yaari, C.J. Cohen, R. Popovtzer, *ACS Nano* **2017** , *11* , 11127.

[20] Y.-P. Zhang, H.-J. Chen, Y. Hu, L. Lin, H.-Y. Wen, D.-W. Pang, S. Zhang, Z.-G. Wang, S.-L. Liu, *Nano Lett* **2024** ,*24* , 1816.

[21] Y. Du, X. Liang, Y. Li, T. Sun, H. Xue, Z. Jin, J. Tian,*Cancer Lett* **2018** , *414* , 230.

[22] Y. Zhang, J. Liu, T.-W. Lo, Y. Kim, F. Lucien, H. Dong, Y. Liu,*Biosens Bioelectron X* **2024** , *19* , 100490.

[23] S. Dey, K.M. Koo, E. Ahmed, M. Trau, *Lab Chip* **2023** , *23* , 3443.

[24] J. Xia, Y. Zhou, Y. Wang, Y. Liu, Q. Chen, K. Koh, X. Hu, H. Chen, *Microchimica Acta* **2024** , *191* , 380.

[25] R.E. Vilain, A.M. Menzies, J.S. Wilmott, H. Kakavand, J. Madore, A. Guminski, E. Liniker, B.Y. Kong, A.J. Cooper, J.R. Howle, R.P.M. Saw, V. Jakrot, S. Lo, J.F. Thompson, M.S. Carlino, R.F. Kefford, G. V Long, R.A. Scolyer, *Clinical Cancer Research* **2017** ,*23* , 5024.

[26] H.Y. Seol, Y.S. Kim, S.-J. Kim, *Thorac Cancer* **2020** , *11* , 3260.

[27] Z. Lin, M. Liu, W. Xing, F. Wang, H. Zhang, X. Wei, H. Schmitthenner, X. Xie, X. Xia, J. Yang, *Biosens Bioelectron* **2023** , *240* , 115633.

[28] Y. Zhang, S. Chen, J. Ma, X. Zhou, X. Sun, H. Jing, M. Lin, C. Zhou, *Anal Chim Acta* **2023** , *1282* , 341927.

[29] A. Bellesoeur, N. Torossian, S. Amigorena, E. Romano,*Curr Opin Chem Biol* **2020** , *56* , 79.

[30] D. Kirschenbaum, K. Xie, F. Ingelfinger, Y. Katzenelenbogen, K. Abadie, T. Look, F. Sheban, T.S. Phan, B. Li, P. Zwicky, I. Yofe, E. David, K. Mazuz, J. Hou, Y. Chen, H. Shaim, M. Shanley, S. Becker, J. Qian, M. Colonna, F. Ginhoux, K. Rezvani, F.J. Theis, N. Yosef, T. Weiss, A. Weiner, I. Amit, *Cell* **2024** , *187* , 149.

[31] Y. Bian, Y. Wang, X. Chen, Y. Zhang, S. Xiong, D. Su,*VIEW* **2023** , *4* , 20220069.

[32] X. Li, G. Chen, K. Wu, H. Zheng, Z. Tian, Z. Xu, W. Zhao, J. Weng, Y. Min, *WIREs Nanomedicine and Nanobiotechnology* **2024** , *16* , e1928.

[33] X. Liu, L. Pan, K. Wang, W. Pan, N. Li, B. Tang, *Chem Sci* **2022** , *13* , 12957.

[34] A. Nguyen, A. Ramesh, S. Kumar, D. Nandi, A. Brouillard, A. Wells, L. Pobezinsky, B. Osborne, A.A. Kulkarni, *Sci Adv* **2024** , *6* , eabc2777.

[35] T. Maj, W. Wang, J. Crespo, H. Zhang, W. Wang, S. Wei, L. Zhao, L. Vatan, I. Shao, W. Szeliga, C. Lyssiotis, J.R. Liu, I. Kryczek, W. Zou, *Nat Immunol* **2017** , *18* , 1332.

[36] D. Sha, Z. Jin, J. Budczies, K. Kluck, A. Stenzinger, F.A. Sinicrope, *Cancer Discov* **2020** , *10* , 1808.

[37] P. Siminzar, M.R. Tohidkia, E. Eppard, N. Vahidfar, A. Tarighatnia, A. Aghanejad, *Mol Imaging Biol* **2023** ,*25* , 464.

[38] A. Passaro, M. Al Bakir, E.G. Hamilton, M. Diehn, F. André, S. Roy-Chowdhuri, G. Mountzios, I.I. Wistuba, C. Swanton, S. Peters,*Cell* **2024** , *187* , 1617.

[39] D.-R. Wang, X.-L. Wu, Y.-L. Sun, *Signal Transduct Target Ther* **2022** , *7* , 331.

[40] D. Daassi, K.M. Mahoney, G.J. Freeman, *Nat Rev Immunol* **2020** , *20* , 209.

[41] C. Wang, C.-H. Huang, Z. Gao, J. Shen, J. He, A. MacLachlan, C. Ma, Y. Chang, W. Yang, Y. Cai, Y. Lou, S. Dai, W. Chen, F. Li, P. Chen,*ACS Sens* **2021** , *6* , 3308.

[42] M. Poggio, T. Hu, C.-C. Pai, B. Chu, C.D. Belair, A. Chang, E. Montabana, U.E. Lang, Q. Fu, L. Fong, R. Blelloch, *Cell* **2019** , *177* , 414.

[43] Y. Zhou, Q. Chen, S. Zhong, H. Liu, K. Koh, H. Chen,*Biosens Bioelectron* **2023** , *237* , 115493.

[44] M. Huang, J. Yang, T. Wang, J. Song, J. Xia, L. Wu, W. Wang, Q. Wu, Z. Zhu, Y. Song, C. Yang, *Angewandte Chemie International Edition* **2020** , *59* , 4800.

[45] C. Sun, R. Mezzadra, T.N. Schumacher, *Immunity* **2018** , *48* , 434.

[46] L. Keren, M. Bosse, D. Marquez, R. Angoshtari, S. Jain, S. Varma, S.-R. Yang, A. Kurian, D. Van Valen, R. West, S.C. Bendall, M. Angelo, *Cell* **2018** , *174* , 1373.

[47] L.A. Walsh, D.F. Quail, *Nat Immunol* **2023** ,*24* , 1982.

[48] P. Lambin, R.T.H. Leijenaar, T.M. Deist, J. Peerlings, E.E.C. de Jong, J. van Timmeren, S. Sanduleanu, R.T.H.M. Larue, A.J.G. Even, A. Jochems, Y. van Wijk, H. Woodruff, J. van Soest, T. Lustberg, E. Roelofs, W. van Elmpt, A. Dekker, F.M. Mottaghy, J.E. Wildberger, S. Walsh, *Nat Rev Clin Oncol* **2017** , *14* , 749.

[49] W. Huang, Y. Jiang, W. Xiong, Z. Sun, C. Chen, Q. Yuan, K. Zhou, Z. Han, H. Feng, H. Chen, X. Liang, S. Yu, Y. Hu, J. Yu, Y. Chen, L. Zhao, H. Liu, Z. Zhou, W. Wang, W. Wang, Y. Xu, G. Li, *Nat Commun* **2022** , *13* , 5095.

[50] L. Devkota, Z. Starosolski, C.H. Rivas, I. Stupin, A. Annapragada, K.B. Ghaghada, R. Parihar, *Sci Adv* **2024** ,*6* , eaba6156.

[51] X.Q. Wang, E. Danenberg, C.-S. Huang, D. Egle, M. Callari, B. Bermejo, M. Dugo, C. Zamagni, M. Thill, A. Anton, S. Zambelli, S. Russo, E.M. Ciruelos, R. Greil, B. Győrffy, V. Semiglazov, M. Colleoni, C.M. Kelly, G. Mariani, L. Del Mastro, O. Biasi, R.S. Seitz, P. Valagussa, G. Viale, L. Gianni, G. Bianchini, H.R. Ali, *Nature* **2023** ,*621* , 868.

[52] D. Fan, Y. Cao, M. Cao, Y. Wang, Y. Cao, T. Gong, *Signal Transduct Target Ther* **2023** , *8* , 293.

[53] B.K. Kashyap, V.V. Singh, M.K. Solanki, A. Kumar, J. Ruokolainen, K.K. Kesari, *ACS Omega* **2023** , *8* , 14290.

[54] Z. Gao, Q. Li, C. Fan, S. Hou, *Sci Bull (Beijing)* **2024** , *69* , 1823.

[55] J. Rong, A. Haider, T.E. Jeppesen, L. Josephson, S.H. Liang,*Nat Commun* **2023** , *14* , 3257.

[56] M. Haris, S.K. Yadav, A. Rizwan, A. Singh, E. Wang, H. Hariharan, R. Reddy, F.M. Marincola, *J Transl Med* **2015** ,*13* , 313.

[57] E. Terreno, D.D. Castelli, A. Viale, S. Aime, *Chem Rev* **2010** , *110* , 3019.

[58] X. Zhang, Y. Wu, L. Chen, J. Song, H. Yang, *Chemical & Biomedical Imaging* **2023** , *1* , 99.

[59] A. Nguyen, A. Ramesh, A. Fish, A.A. Kulkarni, *Adv Funct Mater* **2024** , *n/a* , 2400393.

[60] L. Xu, N. Liu, W. Zhan, Y. Deng, Z. Chen, X. Liu, G. Gao, Q. Chen, Z. Liu, G. Liang, *ACS Nano* **2022** , *16* , 19328.

[61] J. Fu, H. Xi, S. Cai, Y. Peng, Q. Liu, L. Qiu, J. Lin,*ACS Nano* **2024** .

[62] D.A. Mitchell, K.A. Batich, M.D. Gunn, M.-N. Huang, L. Sanchez-Perez, S.K. Nair, K.L. Congdon, E.A. Reap, G.E. Archer, A. Desjardins, A.H. Friedman, H.S. Friedman, J.E. Herndon II, A. Coan, R.E. McLendon, D.A. Reardon, J.J. Vredenburgh, D.D. Bigner, J.H. Sampson,*Nature* **2015** , *519* , 366.

[63] A.J. Grippin, B. Wummer, T. Wildes, K. Dyson, V. Trivedi, C. Yang, M. Sebastian, H.R. Mendez-Gomez, S. Padala, M. Grubb, M. Fillingim, A. Monsalve, E.J. Sayour, J. Dobson, D.A. Mitchell, *ACS Nano* **2019** , *13* , 13884.

[64] T. Sim, B. Choi, S.W. Kwon, K.-S. Kim, H. Choi, A. Ross, D.-H. Kim, *ACS Nano* **2021** , *15* , 12780.

[65] R. Micura, C. Höbartner, *Chem Soc Rev* **2020** ,*49* , 7331.

[66] X. Qin, Y. Xiang, N. Li, B. Wei, Y. Chen, D. Fang, M. Fang, Q. Li, J. Liu, Y. Tang, X. Li, F. Yang, *Biosens Bioelectron* **2022** , *216* , 114636.

[67] Y. Chen, X. Chen, B. Zhang, Y. Zhang, S. Li, Z. Liu, Y. Gao, Y. Zhao, L. Yan, Y. Li, T. Tian, Y. Lin, *Signal Transduct Target Ther* **2024** , *9* , 28.

[68] C.H. Patel, R.D. Leone, M.R. Horton, J.D. Powell, *Nat Rev Drug Discov* **2019** , *18* , 669.

[69] W. Huang, Y. Jiang, W. Xiong, Z. Sun, C. Chen, Q. Yuan, K. Zhou, Z. Han, H. Feng, H. Chen, X. Liang, S. Yu, Y. Hu, J. Yu, Y. Chen, L. Zhao, H. Liu, Z. Zhou, W. Wang, W. Wang, Y. Xu, G. Li, *Nat Commun* **2022** , *13* , 5095.

[70] X.X. Han, R.S. Rodriguez, C.L. Haynes, Y. Ozaki, B. Zhao,*Nature Reviews Methods Primers* **2022** , *1* , 87.

[71] A. Philip, A.R. Kumar, *Coord Chem Rev* **2022** ,*458* , 214424.

[72] S. Ganesh, P. Dharmalingam, S. Das, K. Venkatakrishnan, B. Tan,*ACS Nano* **2023** , *17* , 8026.

[73] Q. Chen, J. Hu, X. Hu, K. Koh, H. Chen, *Biosens Bioelectron* **2022** , *208* , 114179.

[74] J. Li, J. Wang, Y.S. Grewal, C.B. Howard, L.J. Raftery, S. Mahler, Y. Wang, M. Trau, *Anal Chem* **2018** , *90* , 10377.

[75] J. Hu, Z. Zhang, Z. Zhu, J. Chen, X. Hu, H. Chen, *Biosens Bioelectron* **2021** , *185* , 113269.

[76] L. Wang, S. Tang, L. Li, K. Jin, X. Xie, Y. Chen, K. Cai, J. Zhang, *Advanced Sensor Research* **2023** , *2* , 2200062.

[77] X. Du, Y. Li, Z. Zhang, C. Zhang, J. Hu, X. Wang, R. Zhang, J. Yang, L. Zhou, H. Zhang, M. Liu, J. Zhou, *Biosens Bioelectron* **2022** , *207* , 114166.

[78] Y. Cao, Y. Wang, X. Yu, X. Jiang, G. Li, J. Zhao, *Biosens Bioelectron* **2020** , *166* , 112452.

[79] P. Niedziałkowski, M. Bojko, J. Ryl, A. Wcisło, M. Spodzieja, K. Magiera-Mularz, K. Guzik, G. Dubin, T.A. Holak, T. Ossowski, S. Rodziewicz-Motowidło, *Bioelectrochemistry* **2021** ,*139* , 107742.

[80] K. Jin, X. Xie, J. Zhu, Z. Wang, Y. Xing, L. Wang, K. Cai, J. Zhang, *Sens Actuators B Chem* **2023** , *393* , 134191.

[81] J. Li, P.B. Lillehoj, *Angewandte Chemie International Edition* **2022** , *61* .

[82] T. Li, Y. Li, X. Zhu, Y. He, Y. Wu, T. Ying, Z. Xie,*Semin Cancer Biol* **2023** , *91* , 50.

[83] C.C. Smith, S. Chai, A.R. Washington, S.J. Lee, E. Landoni, K. Field, J. Garness, L.M. Bixby, S.R. Selitsky, J.S. Parker, B. Savoldo, J.S. Serody, B.G. Vincent, *Cancer Immunol Res* **2019** ,*7* , 1591.

[84] P. Borole, A. Rajan, *Commun Biol* **2024** ,*7* , 279.

[85] X. He, J. Li, J. Xu, H. Shan, S. Shen, S. Gao, H.E. Xu,*Acta Pharmacol Sin* **2024** .

[86] O. Méndez-Lucio, M. Ahmad, E.A. del Rio-Chanona, J.K. Wegner,*Nat Mach Intell* **2021** , *3* , 1033.

[87] K.A. Tran, O. Kondrashova, A. Bradley, E.D. Williams, J. V Pearson, N. Waddell, *Genome Med* **2021** , *13* , 152.

[88] J. van der Laak, G. Litjens, F. Ciompi, *Nat Med* **2021** , *27* , 775.

[89] K. Bera, N. Braman, A. Gupta, V. Velcheti, A. Madabhushi,*Nat Rev Clin Oncol* **2022** , *19* , 132.